

# Radiated Power Evaluation of Simulated Radio Equipment Using Equi-Spaced-Points-Method

#Nozomu Ishii<sup>1</sup>

<sup>1</sup> Faculty of Engineering, Niigata University  
8050, Ikarashi 2-nocho, Nishi-ku, Niigata, 950-2181, Japan  
nishii@eng.niigata-u.ac.jp

## 1. Introduction

In 2003, a method of measurement for radiated RF power and receiver performance was proposed by CTIA. In the certification [1], it is recommended that radiation characteristics in real operative state should be evaluated. Although maximal EIRP has been used to obtain radiated power of radio equipments, it cannot always indicate their performance in real operative state. Therefore, CTIA certification [1] describes that total radiation power (TRP), which is radiated by radio equipment, should be measured to evaluate transmitter performance.

As shown in Fig. 1, a given radio equipment is located near the origin of the spherical coordinate system. As EIRP does not depend upon the distance,  $r$ , in the far-field region, TRP is evaluated by integrating the sum of EIRPs for vertical and horizontal polarizations,  $\text{EIRP}(\theta, \phi) = \text{EIRP}_\theta(\theta, \phi) + \text{EIRP}_\phi(\theta, \phi)$ , over the entire unit spherical surface [1][2].

$$\text{TRP} = \frac{1}{4\pi} \int_0^{2\pi} \int_0^\pi \text{EIRP}(\theta, \phi) \sin\theta d\theta d\phi = \frac{\pi}{2N_\theta N_\phi} \sum_{i=1}^{N_\theta} \sum_{j=1}^{N_\phi} \text{EIRP}(\theta_i, \phi_j) \sin\theta_i, \quad (1)$$

where  $\theta_i = i\Delta\theta = i(\pi/N_\theta)$ ,  $\phi_j = j\Delta\phi = j(2\pi/N_\phi)$  are angular intervals and  $N_\theta$  and  $N_\phi$  are division numbers in the  $\theta$  and  $\phi$  directions. For example, the angular intervals should be at least less than  $15^\circ$  in [1], which corresponds to  $N_\theta = 12$ ,  $N_\phi = 24$  so that it is required that EIRPs be measured at 288 points. Furthermore, the radiation pattern of the radio equipment including antennas is not simple as an eight-shape but complex in that the polarization is tilted and the shape of the lobe is constricted. In addition, the pattern is more complex and the power level of higher harmonic frequencies is very low for spurious radiation.

In the summation in (1), sampling angles for  $\theta$  and  $\phi$  are uniformly divided, and then there is a problem that area of divided region is smaller at rate of  $\sin\theta$  as  $\theta$  approaches 0 or  $\pi$ . Although the correction factor of  $\sin\theta$  is considered in the integration, the number of sampling per unit area near  $\theta = \pi/2$  is different from that near  $\theta = 0, \pi$ . To solve this difficulty, an equi-spaced-points-method (ESPM) was proposed and was numerically examined by use of known and explicit functions of the radiation intensity [3]. Although it has mechanical and graphical disadvantages, it can evaluate the integrand with no weight at the sampling points.

In this paper, radiated power of a simulated radio equipment including antennas will be evaluated by use of ESPM, in which the sampling points can be selected as the same weight per unit area and then the radiation intensity is numerically integrated over entire unit spherical surface. The results by use of ESPM will be compared with that of conventional equi-angle division.

## 2. Review of Equi-Area Division Algorithm

An equi-area division algorithm used in this paper is based on the recursive algorithm for multi-dimensional spherical surface proposed by P. Leopardi [4]. Let us consider a spherical surface with  $r = 1$ . Its center is located at the origin of the spherical coordinate system  $(r, \theta, \phi)$  as shown in Fig. 1. In the equi-area division, when total division number  $N$  is given, division number in the  $\theta$  direction,  $n$ , is determined, and then division number in the  $\phi$  direction for each collar region  $R_{c,i}$ ,  $m_i$ , is determined as divided regions have nearly equal area. The procedure is described as below.

- (1) The spherical surface is divided into two polar cap regions whose centers are located at  $\theta = 0, \pi$  and several collar regions between the cap regions.

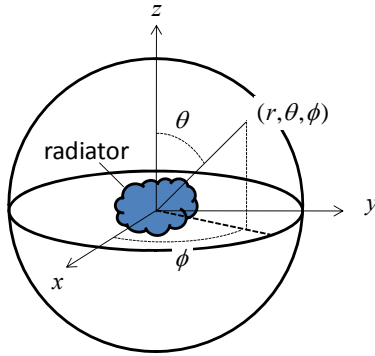


Figure 1: A Radiator in Spherical Coordinate System

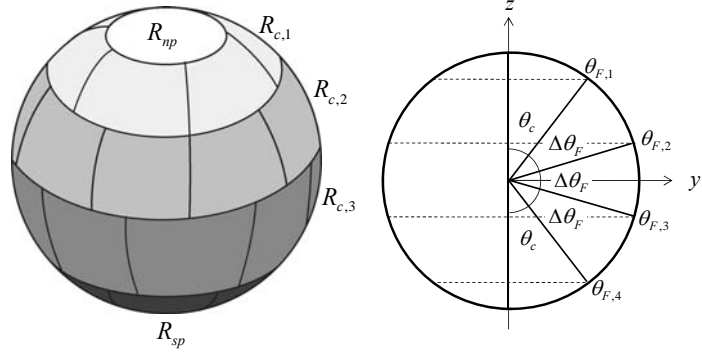


Figure 2: An Example of Equi-Areas Divided by Equi-Area Division Algorithm

- (2) The range of the cap regions  $R_{np}, R_{sp}$ ,  $0 < \theta < \theta_c$  and  $\pi - \theta_c < \theta < \pi$ , is determined.
- (3) The number of the collar region,  $n$ , is determined. ( $n\Delta\theta_F = \pi - 2\theta_c$ )
- (4) The division number for each collar region  $R_{c,i}$ ,  $m_i$ , is determined. ( $m_i\Delta\phi_i = 2\pi$ )
- (5) The sampling point or central point for each equi-area region ( $\theta_{s,i}, \phi_{s,(i,j)}$ ) is determined.
- (6) The radiation intensity  $U(\theta, \phi)$  is numerically summed up at the above sampling points to obtain the radiated power,  $P_r$ .

In practice, the divided equi-area regions do not have exactly equal area so that the surface integral should be approximated as

$$P_r = \int_0^{2\pi} \int_0^\pi U(\theta, \phi) \sin\theta d\theta d\phi \approx \sum_{i=1}^{n+1} \sum_{j=1}^{m_i} U(\theta_{s,i}, \phi_{s,(i,j)}) A_{ij}, \quad (2)$$

where  $A_{ij} = \sin\theta_{s,i} \Delta\theta_F \Delta\phi_i$  is area of the equi-area region ( $\theta_{s,i}, \phi_{s,(i,j)}$ ). When TRP is evaluated,  $P_r$  and  $U(\theta, \phi)$  should be replaced as TRP and  $\text{EIRP}(\theta, \phi)/4\pi$  in (2), respectively

### 3. Simulated Radio Equipments

Radiation patterns of a simulated radio equipment shaped like a notebook sized PC were measured as a function of the elevation and azimuth angles by Telecom Engineering Center (TELEC), Japan [5]. A measurement system for spherical radiation pattern that is taken in canonical cut system had developed by TELEC. The center of the notebook sized PC was located at the origin of the spherical coordinate system. The equipment has a fundamental harmonic with 2.412GHz, and the radiation patterns related to the fundamental, second and third harmonics were measured. The angular intervals are listed in Table 1. In this paper, the angular data of the radiation pattern are assumed to be given so that the measurement equipment, the procedure of the calibration, and so on, will not be discussed.

## 4. Evaluation of Total Radiation Power

### 4.1 Selection of Sampling Points

In the case of evaluating a whole radiated power  $P_r$  by use of the equi-area division, the most accurate way to obtain the radiation power is to select central points of the equi-area regions ( $\theta_{s,i}, \phi_{s,(i,j)}$ ) as sampling points. However, in a rigorous sense, there are no measured data at the central points assigned by the equi-area division algorithm because the data used in this paper are gathered at the angular intervals listed in Table 1. For example, Table 2 lists  $\theta_{s,i}$  and  $\Delta\phi_i$  for the division number of  $N = 200$ . It can be found that a lot of equi-area regions are assigned near  $\theta = 90^\circ$ , but a few are assigned near  $\theta = 0^\circ$  or  $180^\circ$ . On the other hand,  $\Delta\theta_F \approx 15^\circ$  and  $\Delta\phi_i \approx 15^\circ$  near the equator of the unit spherical surface so that this division number  $N = 200$  is about 0.7 times as large as that for equi-angle division, i.e.  $N_\theta \times N_\phi = 12 \times 24 = 288$ .

In this paper, the division number is so large that area of the divided regions is infinitesimal, and then the data at the center in the region can be replaced by the data included in the region.

Table 1: Angular Intervals of Given Data

Frequency	Angular Interval	
	$\Delta\theta$	$\Delta\phi$
2.412 GHz	5°	1°
4.824 GHz	1°	1°
7.236 GHz	1°	1°

Table 2: An Example of Sampling Point by Equi-Area Division Algorithm,  $N = 200$

$i$	$\theta_{s,i}$	$m_i$	$\Delta\phi_i$	$i$	$\theta_{s,i}$	$m_i$	$\Delta\phi_i$
0	0°	1	180°	7	104.9°	25	14.4°
1	15.6°	7	51.4°	8	119.8°	22	16.4°
2	30.4°	13	27.7°	9	134.7°	19	18.9°
3	45.3°	19	18.9°	10	149.6°	13	27.7°
4	60.2°	22	16.4°	11	164.4°	7	51.4°
5	75.1°	25	14.4°	12	180°	1	180°
6	90.0°	26	13.8°	$n = 11, \Delta\theta_F = 14.9^\circ$			

Of course, as the division number decreases, this approximation becomes worse. That is, the uncertainty due to selecting the sampling points should be considered if the division number is not large. Anyway, it is necessary to recognize that the sampling points assigned by the equi-area division algorithm do not correspond to those for the equi-angle division.

#### 4.2 Surface Integral Evaluation by Use of Equi-Angle Division

Table 3 shows the radiated power,  $P_r$ , integrated by use of (1), or the equi-angle division as a function of the division number. When angle interval is less than 15°, or the division number is more than 288, the integral value almost converges. For measured frequency except fundamental harmonic, the difference of the integral values for angle interval of between 1° and 5° is less than 0.02dB and the difference between 1° and 15° is less than 0.12dB [5].

#### 4.3 Surface Integral Evaluation by Use of Equi-Area Division

Tables 4-6 show the radiated power,  $P_r$ , integrated by use of (2), or the equi-area division, as a function of the division number,  $N$ . As shown in Table 2, the angle intervals are not 1°. In practice, the number of sampling points should be reduced if the accuracy can be ensured because of saving measurement time. In Tables 4-6, the surface integral is evaluated by three ways of data selection, (i)  $\Delta\theta_m = \Delta\phi_m = 15^\circ$ , (ii)  $\Delta\theta_m = \Delta\phi_m = 5^\circ$ , (iii)  $\Delta\theta_m = 5^\circ$  or  $1^\circ$ ,  $\Delta\phi_m = 1^\circ$ , where it is assumed that the data exist only at interval of  $\Delta\theta_m$  and  $\Delta\phi_m$  in the  $\theta$  and  $\phi$  directions. In the case of (iii), the surface integral is evaluated by making full use of the data. It is found that the integral value by the equi-area division gives close agreement with that by the equi-angle division by comparing Table 3 with Table 6.

In the equi-area division, the integral value converges as the division number,  $N$ , increases. The reason why the convergence is not monotonic is that discrete operations are included in determining the equi-area divisions and the sampling points are not always the central points of the equi-area region assigned by the algorithm. If the error of 0.2dB is permitted,  $N = 300$  is enough for the division number in the case of (iii). Note that the division number is enormous as the angle interval is smaller so that the measurement is practically impossible for the equi-angle division. In this sense, the division number of  $N = 300$  for the equi-area division leads to realistic measurements in the view of saving the measurement time.

As seen from Table 4, in the case of (i)  $\Delta\theta_m = \Delta\phi_m = 15^\circ$ , the radiated power almost converges as the division number,  $N$ , increases, however, is a little poorly-converged especially for the fundamental harmonic, in comparison to the cases (ii) and (iii) related to Tables 5 and 6. The reasons include the radiated pattern is complex because of using the integrated radio equipment and the value of the numerical integral fluctuates when the angle intervals are coarser. On the other hand, in the case of (ii)  $\Delta\theta_m = \Delta\phi_m = 5^\circ$ , the convergence of the numerical integral is good as the division number increases and bears comparison with the case of (iii).

## 5. Conclusions

In this paper, the equi-area division algorithm to evaluate the radiated power was examined for the simulated radio equipment shaped like a notebook sized PC. When the division number is rather large, the surface integral can be evaluated by use of the measured data near the sampling points assigned by the algorithm. By selecting appropriate angle intervals of given data, the integral values are almost same as those by use of the equi-angle division. The radiation intensity or EIRP

Table 3: Radiated Power Evaluated by use of  
Equi-Angle Division

N	$\Delta\theta$	$\Delta\phi$	$P_r$ [dBm]		
			2.412GHz	4.812GHz	7.236GHz
32	45°	45°	1.23	-49.58	-62.22
72	30°	30°	1.46	-49.56	-61.08
162	20°	20°	1.30	-49.87	-61.10
288	15°	15°	1.42	-49.58	-61.27
648	10°	10°	1.38	-49.63	-61.21
2592	5°	5°	1.37	-49.68	-61.29
16200	2°	2°	-	-49.69	-61.31
64800	1°	1°	-	-49.70	-61.31

Table 4: Radiated Power Evaluated by use of  
Equi-Area Division in the case of  
(i)  $\Delta\theta_m = \Delta\phi_m = 15^\circ$

N	$P_r$ [dBm]		
	2.412GHz	4.812GHz	7.236GHz
100	1.60	-49.44	-61.26
200	1.43	-49.68	-61.20
300	1.34	-49.61	-61.17
400	1.48	-49.42	-61.23
500	1.45	-49.59	-61.16
600	1.43	-49.62	-61.21
700	1.38	-49.60	-61.33
800	1.47	-49.56	-61.17
900	1.44	-49.51	-61.22
1000	1.45	-49.51	-61.28

Table 5: Radiated Power Evaluated by use of  
Equi-Area Division in the case of  
(ii)  $\Delta\theta_m = \Delta\phi_m = 5^\circ$

N	$P_r$ [dBm]		
	2.412GHz	4.812GHz	7.236GHz
100	1.37	-49.86	-60.68
200	1.41	-49.55	-61.25
300	1.40	-49.75	-61.44
400	1.39	-49.68	-61.11
500	1.37	-49.67	-61.31
600	1.39	-49.67	-61.27
700	1.37	-49.68	-61.24
800	1.41	-49.62	-61.26
900	1.36	-49.78	-61.22
1000	1.38	-49.62	-61.26

Table 6: Radiated Power Evaluated by use of  
Equi-Area Division in the case of  
(iii)  $\Delta\theta_m = 5^\circ$  or  $1^\circ$ ,  $\Delta\phi_m = 1^\circ$

N	$P_r$ [dBm]		
	2.412GHz	4.812GHz	7.236GHz
100	1.37	-49.88	-60.92
200	1.43	-49.52	-61.13
300	1.42	-49.67	-61.45
400	1.37	-49.72	-61.19
500	1.39	-49.68	-61.28
600	1.38	-49.70	-61.27
700	1.38	-49.69	-61.36
800	1.42	-49.67	-61.25
900	1.37	-49.68	-61.30
1000	1.39	-49.67	-61.25

does not have to be an explicit function of  $\theta$  and  $\phi$  and its pattern does not have to be simple. Even if measured radiation pattern are given, it is possible to evaluate the surface integral for the radiated wave with a complex pattern and the convergence of the integral is stable as the division number increases. However, the convergence depends upon the angle interval of the radiation pattern, and at this stage the equi-area division is not always superior to the equi-angle division.

## Acknowledgments

The measured data used in this paper are cited from the research project of TELEC, Japan, "R&D on quick and accurate measurement techniques for the radiated power" supported by the Ministry of Internal Affairs and Communications, Japan.

## References

- [1] CTIA certification: Test plan for mobile station over the air performance - method of measurement for radiated RF power and receiver performance, revision number 2.2.2, Dec. 2008.
- [2] C. A. Balanis, *Antenna Theory Analysis and Design*, 3rd edition, Wiley, 2005.
- [3] S. Ullah, J. A. Flint, and R. D. Seager, "Equi-spaced-points-method (ESPM) for antenna radiation pattern (ARP) measurements with 3D-rotation," *Proc. EuCAP 2007*, Th2.11.6, Edinburgh, UK, Nov. 2007.
- [4] P. Leopardi, "A partition of the unit sphere into regions of equal area and small diameter," *Electronic Transactions on Numerical Analysis*, Vol. 25, pp.309-327, 2006.
- [5] T. Watanabe, K. Nakajima, T. Shigeno, and H. Arai, "Total radiated power measurement for a portable transmitter using spherical and hemispherical scanning," *IEICE Technical Report*, ACT2008-13, pp.6-11, Kyoto, Japan, Dec. 2008. (written in Japanese)